Modulated electrostatic modes in pair plasmas: modulational stability profile and envelope excitations

I. Kourakis[a,1], A. Esfandyari-Kalejahi[b,2], M. Mehdipoor[b] and P.K. Shukla [a,3]

[a] *Ruhr-Universität Bochum, Institut fürTheoretische Physik IV,*
Fakultät für Physik und Astronomie, D-44780 Bochum, Germany.

[b] *Azarbaijan University of Tarbiat Moallem, Faculty of Science,*
Department of physics, 51745-406, Tabriz, Iran.

Email: [1] ioannis@tp4.rub.de, [2] ra-esfandyari@azaruniv.edu, [3] ps@tp4.rub.de

Submitted 5 January 2006; revised 11 April 2006

Abstract

A pair plasma consisting of two types of ions, possessing equal masses and opposite charges, is considered. The nonlinear propagation of modulated electrostatic wave packets is studied, by employing a two-fluid plasma model. Considering propagation parallel to the external magnetic field, two distinct electrostatic modes are obtained, namely a quasi-acoustic lower mode and a Langmuir-like optic-type upper one, in agreement with experimental observations and theoretical predictions. Considering small yet weakly nonlinear deviations from equilibrium, and adopting a multiple-scale technique, the basic set of model equations is reduced to a nonlinear Schrödinger (NLS) equation for the slowly varying electric field perturbation amplitude. The analysis reveals that the lower (acoustic) mode is stable and may propagate in the form of a dark-type envelope soliton (a void) modulating a carrier wave packet, while the upper linear mode is intrinsically unstable, and may favor the formation of bright-type envelope soliton (pulse) modulated wavepackets. These results are relevant to recent observations of electrostatic waves in pair-ion (fullerene) plasmas, and also with respect to electron-positron plasma emission in pulsar magnetospheres.

PACS Nos: 52.30.Ex, 52.27.Ep, 52.35.Fp, 52.35.Mw.

Keywords: Pair plasmas, electrostatic plasma modes, amplitude modulation, nonlinear Schrödinger equation (NLSE), modulational instability, envelope solitons.

I. Introduction

Increasing interest has recently been drawn to the properties of *pair plasmas*, i.e. fully ionized plasmas consisting of two populations of different charge signs, possessing equal mass and absolute charge values ($m_1 = m_2 = m$, $q_1 = -q_2 = +Ze$). Magnetized electron-positron (e-p) plasmas exist in pulsar magnetospheres [1-5], in bipolar outflows (jets) in active galactic nuclei [6], at the center of our own galaxy [7], in the early universe [8], and in inertial confinement fusion scheme using ultra-intense lasers [9]. Recently, the possibility of pair production in large tokamaks due to collisions between multi-MeV runaway electrons and thermal particles was discussed [10]. A number of pioneering experiments carried out hardly more than a decade ago [11-14] have enabled the production of positron plasmas in laboratory, thus opening the road to experimental studies of electron-positron plasmas. More recently, the production of pair fullerene-ion plasmas [15-17] has enabled experimental studies of pair plasmas rid of intrinsic problems involved in electron-positron plasmas, namely pair recombination processes and strong Landau damping.

The physics of pair plasmas is remarkably different from that of electron-ion (e-i) plasmas. In specific, contrary to ordinary plasmas, which are characterized by distinct frequency scales as imposed by the large mass mismatch between electrons and ions [18, 19], pair plasmas are bereft of such a scale separation, hence featuring a variety of challenging new physical phenomena, which include novel possibilities for interaction among electromagnetic modes, and absence of Faraday rotation, to mention only a few. Various theoretical studies of linear electrostatic and electromagnetic pair plasma modes have been carried out, adopting either a kinetic [20-22] or a fluid dynamical [23, 24] approach, while a number of theoretical studies have been devoted to nonlinear [25-28] excitations in pair plasmas, as well as in pair-ion (e.g. electron-positron-ion) plasmas [29].

Focusing on electrostatic waves propagating parallel to the magnetic field, two distinct modes have been observed in fullerene experiments [16, 17] on equal

temperature ($T_- = T_+ = T$) pair plasmas. These consist of a thermal mode $\omega_1 = k\,c_s$ (here ω_1, k and $c_s \sim (T/m)^{1/2}$ refer to the frequency, wavenumber and ion thermal speed, respectively), and a Langmuir-analogue dispersive optic-type electrostatic mode $\omega_2^2 = 2\omega_p^2 + k^2 c_s^2$, featuring a cutoff frequency $\omega_2(k=0) = \sqrt{2}\,\omega_p$ (here ω_p is the common value of the characteristic plasma frequency, corresponding to the negative or positive ions). The former (thermal) mode obviously suffers strong damping, due to Landau resonance among the neighboring values of phase and thermal speeds.

The present study is devoted to an investigation of the modulational stability profile of parallel propagating electrostatic modes in pair plasmas. Relying on a two-fluid plasma model and adopting a slowly varying amplitude hypothesis, we shall employ a multiple-scale technique [30-32] in order to derive a nonlinear Schrödinger- (NLS) type evolution equation [33] for the amplitude of weakly nonlinear electrostatic perturbations from equilibrium. The amplitude's (modulational) stability will then be studied, and the anticipated occurrence of modulated envelope excitations will be discussed. The outline of the article goes as follows. The analytical model is presented in Section II. A reductive perturbation theory is employed in Section III, to obtain a NLS equation for the electric field amplitude, whose stability profile is analyzed in Section IV. The possibility for the formation of propagating electrostatic envelopes in pair plasmas is suggested in Section V, where analytical expressions for these localized envelope modes are provided. Finally, our results are summarized in Section VI.

II. The model equations

We consider a plasma consisting of two particle species, say 1 and 2, of opposite charge signs, characterized by equal masses and equal absolute charges, i.e. $q_1 = -q_2 = +Ze$, $m_1 = m_2 = m$. In specific, this picture applies to the pair fullerene-ion plasmas recently created in laboratory [15-17], as well as electron-positron plasmas, for $Z = 1$.

The two-fluid plasma-dynamical equations for a pair plasma include the density evolution equation

$$\frac{\partial n_\alpha}{\partial t} + \vec{\nabla}.(n_\alpha \vec{u}_\alpha) = 0\,, \tag{1}$$

and the momentum equation

$$\frac{\partial \vec{u}_\alpha}{\partial t} + (u_\alpha.\vec{\nabla})\vec{u}_\alpha = -\frac{q_\alpha}{m_\alpha}\vec{\nabla}\phi - \frac{\vec{\nabla}p_\alpha}{m_\alpha n_\alpha}\,, \tag{2}$$

where the Lorentz force term is neglected, since wave propagation parallel to an external magnetic field is assumed. The subscript α denotes either species 1 (i.e. the positive ions, or positrons) for $\alpha = +$, or species 2 (i.e. the negative ions, or electrons) for $\alpha = -$. The moment variables n_α and $\vec{U}_\alpha$ denote the density and velocity of species α, respectively. The potential ϕ is determined by the Poisson equation

$$\nabla^2\phi = 4\pi e Z(n_- - n_+) \quad , \tag{3}$$

where the right-hand side is assumed to cancel at equilibrium, viz. $n_{-,0} = n_{+,0} = n_0$. The system of Eqs. (1) to (3) is closed by assuming an explicit density dependence of the pressure in the form $p_\alpha = C n_\alpha{}^\gamma$, where γ is the ratio of specific heats. Combining this assumption with the equation of state (at equilibrium) $p_{\alpha,0} = \gamma n_{\alpha,0} k_B T_\alpha$ (where T_α denotes the temperature of species α; k_B is Bolztmann's constant), the pressure term may be rearranged as $\left(\vec{\nabla}p_\alpha\right)/n_\alpha = \gamma K_B T_\alpha n_{\alpha 0}{}^{1-\gamma} n_\alpha{}^{\gamma-2}\vec{\nabla}n_\alpha$.

The model equations may be cast into a reduced (dimensionless) form by scaling the time and space variables as $t' \equiv \omega_p t$ and $x' \equiv x/\lambda_{D,-}$, respectively, where the characteristic scales are defined by the plasma frequency $\omega_{p,\alpha} = (4\pi n_0 q_\alpha^2/m_\alpha)^{1/2}$ (see

that $\omega_{p,-} = \omega_{p,+} = \omega_p$) and the Debye frequency $\lambda_{D,\alpha} = \left(K_B T_\alpha / m\,\omega_{p,\alpha}\right)^{1/2}$ (note that $\lambda_{D,-} = \lambda_{D,+}$ if $T_- = T_+$). The density, velocity and electric potential state variables are scaled as $n'_\alpha = n_\alpha / n_0$, $u'_\alpha = u_\alpha / c_s$ and $\phi' = \phi / \phi_0$, respectively, where we have defined the characteristic (thermal) speed $c_s = \left(K_B T_- / m\right)^{1/2}$ (for negative ions) and the characteristic potential scale $\phi_0 = K_B T_- / Ze$ (the primes will be dropped for simplicity). Combining these definitions and considering a one-dimensional geometry (along x), the model equations reduce to

$$\frac{\partial n_\alpha}{\partial t} + \frac{\partial (n_\alpha u_\alpha)}{\partial x} = 0 \ , \tag{4}$$

$$\frac{\partial u_\alpha}{\partial t} + u_\alpha \frac{\partial u_\alpha}{\partial x} = -s_\alpha \frac{\partial \phi}{\partial x} - \gamma \sigma_\alpha n_\alpha^{\gamma-2} \vec{\nabla} n_\alpha \ , \tag{5}$$

and

$$\nabla^2 \phi = n_- - n_+ \ , \tag{6}$$

where we have defined the dimensionless parameter $s_\alpha = q_\alpha / |q_\alpha| = +1/-1$, which denotes the charge sign of species α, and the temperature ratio $\sigma_\alpha = T_\alpha / T_-$. In the following, we shall explicitly consider that $\gamma = 3$ (for one degree of freedom) and $\sigma_- = \sigma_+ = 1$, i.e. $T_- = T_+$, in accordance with experimental considerations [15-17]. Nevertheless, we have chosen to keep the parameter $\sigma = \sigma_+ = T_+ / T_-$ appearing in forthcoming formula, for generality. The model equations thus define a closed set of five coupled equations, which will be used as a basis for the analysis that follows.

III. Perturbative analysis - the nonlinear Schrödinger equation

In order to obtain an explicit evolution equation describing the propagation of modulated waves, relying on the model equations introduced above, we shall employ the standard reductive perturbation (multiple scales) technique [30-32], which consists in stretching the independent variables x and t as $\xi = \varepsilon(x - \lambda t)$ and $\tau = \varepsilon^2 t$, where $\varepsilon << 1$ is a (dimensionless) smallness parameter and λ is a real parameter, to be later determined by compatibility requirements. The state variables are expanded as

$$n_\alpha = 1 + \sum_{n=1}^{\infty} \sum_{l=-\infty}^{+\infty} \varepsilon^n \; n_{\alpha,l}^{(n)}(\xi,\tau)\, e^{il(kx-\omega t)}$$

$$u_\alpha = \sum_{n=1}^{\infty} \sum_{l=-\infty}^{\infty} \varepsilon^n \; u_{\alpha,l}^{(n)}(\xi,\tau)\, e^{il(kx-\omega t)}$$

and

$$\phi = \sum_{n=1}^{\infty} \sum_{l=-\infty}^{\infty} \varepsilon^n \phi_l^{(n)}(\xi,\tau) e^{il(kx-\omega t)} \quad . \tag{7}$$

where the reality condition $A_{-l}^{(n)} = A_l^{(n)*}$ is met by the amplitudes $A_l^{(n)} \in \{n_{\alpha,l}^{(n)}, u_{\alpha,l}^{(n)}, \phi_l^{(n)}\}$ of all state variables; the asterisk superscript denotes the complex conjugate (c.c.). Substituting the expansion ansatz (7) into the model equations (4)-(6), and then isolating distinct orders in ε, we obtain the nth order reduced equations:

$$-\lambda \frac{\partial n_{\alpha,l}^{(n-1)}}{\partial \xi} + \frac{\partial n_{\alpha,l}^{(n-2)}}{\partial \tau} - il\omega n_{\alpha,l}^{(n)} + ilkU_{\alpha,l}^{(n)} + \frac{\partial U_{\alpha,l}^{(n-1)}}{\partial \xi} + \sum_{n'=1}^{\infty} \sum_{l'=-\infty}^{\infty} [ilkn_{\alpha,l'}^{(n')} U_{\alpha,l-l'}^{(n-n')} + \frac{\partial}{\partial \xi}(n_{\alpha l'}^{(n')} U_{\alpha,l-l'}^{(n-n'-1)})] = 0 \, ,$$

$$\frac{\partial u_{\alpha,l}^{(n-2)}}{\partial \tau} - \lambda \frac{\partial u_{\alpha,l}^{(n-1)}}{\partial \xi} - il\omega u_{\alpha,l}^{(n)} + \sum_{n'=1}^{\infty} \sum_{l'=-\infty}^{\infty} [il'ku_{\alpha,l-l'}^{(n-n')} u_{\alpha,l'}^{(n')} + u_{\alpha,l-l'}^{(n-n'-1)} \frac{\partial u_{\alpha,l'}^{(n')}}{\partial \xi}]$$
$$= -s_\alpha \frac{\partial \phi_l^{(n-1)}}{\partial \xi} - s_\alpha ilk\phi_l^{(n)} - \gamma\, i\, \sigma_\alpha\, lkn_{\alpha,l}^{(n)} - \gamma\, \sigma_\alpha \frac{\partial n_{\alpha,l}^{(n-1)}}{\partial \xi} - \gamma\, \sigma_\alpha \sum_{n'=1}^{\infty} \sum_{l'=-\infty}^{\infty} [il'n_{\alpha,l-l'}^{(n-n')}\, k\, n_{\alpha,l'}^{(n')} + n_{\alpha,l-l'}^{(n-n'-1)} \frac{\partial n_{\alpha,l'}^{(n')}}{\partial \xi}] \quad ,$$

and

$$\frac{\partial^2 \phi_l^{(n-2)}}{\partial \xi^2} - l^2 k^2 \phi_l^{(n)} + 2ilk \frac{\partial \phi_l^{(n-1)}}{\partial \xi} = n_{-,l}^{(n)} - n_{+,l}^{(n)} \quad , \tag{8}$$

where $\alpha = +,-$ denotes the two particle species present; recall that $s_+ = -s_- = +1$.

The first-order (for n=1) equations read

$$-il\omega n_{-,l}^{(1)} + ilku_{-,l}^{(1)} = 0 \ ,$$

$$-il\omega n_{+,l}^{(1)} + ilku_{+,l}^{(1)} = 0 \ ,$$

$$-il\omega u U_{-,l}^{(1)} = ilk\varphi_l^{(1)} - \gamma ilkn_{-,l}^{(1)} \ ,$$

$$-il\omega u_{+,l}^{(1)} = -ilk\phi_l^{(1)} - \gamma\sigma\, i\, lkn_{+,l}^{(1)} \quad ,$$

and

$$-l^2k^2\phi_l^{(1)} = n_{-,l}^{(1)} - n_{+,l}^{(1)} \quad . \tag{9}$$

(the γ notation was temporarily recovered, for generality; γ=3 is nevertheless understood). For l=1 the following dispersion relation is deduced

$$\omega^4 - \left[2 + \gamma(1+\sigma)k^2\right]\omega^2 + \gamma k^2(\gamma\sigma k^2 + 1 + \sigma) = 0 \tag{10}$$

Two real solutions are thus obtained for the (squared) frequency ω^2, defined by

$$\omega_1^2 = 1 + \frac{\gamma}{2}(1+\sigma)k^2 - \sqrt{1 + \frac{\gamma^2}{4}k^4(1-\sigma)^2} \tag{11a}$$

and

$$\omega_2^2 = 1 + \frac{\gamma}{2}(1+\sigma)k^2 + \sqrt{1 + \frac{\gamma^2}{4}k^4(1-\sigma)^2} \quad . \tag{11b}$$

For small k, these branches behave as

$$\omega_1^2 \approx \gamma(1+\sigma)k^2/2 \tag{12a}$$

and

$$\omega_2^2 \approx 2 + \gamma(1+\sigma)k^2/2 \quad , \tag{12b}$$

i.e. recovering dimensions, $\omega_1^2 \approx \gamma(1+\sigma)\, c_s^2\, k^2/2$ and $\omega_2^2 \approx 2\omega_p^2 + \gamma(1+\sigma)\, c_s^2\, k^2/2$; a characteristic speed $c_0 = c_s\sqrt{\gamma(1+\sigma)/2}$ is thus defined. Electrostatic modes in pair-ion plasmas therefore include a *thermal* dispersion, $\omega_1 \approx \pm k\, c_o$, and a Langmuir-like optical behavior $\omega_2 \approx \pm\sqrt{2\omega_p^2 + k^2 c_0^2}$, for small k. For clarity, $\omega = \omega_1$ and $\omega = \omega_2$ will henceforth be referred to as the lower and the upper curve, respectively. Note that, for $\sigma = 1$ (i.e. $T_- = T_+$), one obtains the exact expressions $\omega_1^2 = \gamma k^2$ and $\omega_2^2 = 2 + \gamma k^2$, or recovering dimensions,

$$\omega_1^2 = \gamma k^2 c_s^2 \tag{13a}$$

and

$$\omega_2^2 = 2\,\omega_p^2 + \gamma k^2\, c_s^2 \tag{13b}$$

Note, for rigor, that the former branch has been argued to be subject to strong damping, due to the phase speed ω_1/k being extremely close to the ion thermal speed [20]. The two dispersion curves obtained here are depicted in Figure 1. The results presented in this paragraph are in full agreement with (and in fact generalize, for arbitrary σ) known experimental [16, 17] and theoretical [24] results.

A brief technical comment is in order here. Once a compatibility condition in the explicit form of Eq. (10) is fulfilled, which is in fact tantamount to requiring that the 5x5 homogeneous system of Eqs. (9) possesses a vanishing determinant $D = 0$ and thus has a non-trivial solution, then the system obeyed by the first-order perturbation harmonics may be either simply or multiply non-determinate. In the former case, 4 of the sought parameters may be determined in terms of the 5th (say, the electric potential $\phi_1^{(1)}$), as is usually the case when the reductive perturbation technique employed here is adopted (see e.g. in Ref. [32]). In the latter case, e.g. if the system is two-fold indeterminate, then 3 of the sought parameters may be determined in terms of the 4th and 5th ones (say, in terms of the electric potential $\phi_1^{(1)}$ and the ion density $n_1^{(1)}$). Which the case is, needs to be carefully investigated, in terms of the (determinant of the) reduced 4x4 *inhomogeneous* linear system obtained by omitting, say (with no loss of generality), the 5th equation in (9). The determinant of the 4x4 reduced matrix thus obtained reads

$D_0 = \left(\omega^2 - \gamma\sigma k^2\right)\left(\omega^2 - \gamma k^2\right)$, so the 1st order 1st harmonic system will be only *simply* indeterminate *if (and only if)* $\omega^2 \neq \gamma k^2$ *and* $\omega^2 \neq \gamma\sigma k^2$. This condition *is* indeed satisfied, unless $\sigma = 1$ is assumed, and the lower (thermal) branch $\omega = \omega_1$ given by (12a) is considered. Note that the dispersion relation (10) then takes the simple form

$$\frac{1}{\omega^2 - \gamma\sigma k^2} + \frac{1}{\omega^2 - \gamma k^2} = 1.$$

Therefore, one needs to distinguish the case

(i) $\sigma = 1$, and the lower (thermal) curve $\omega = \omega_1$ given by (12a) is considered,

from the case(s) when either

(ii) $\sigma = 1$, and the upper curve $\omega = \omega_2$ given by (12b) is considered ,

or

(iii) $\sigma \neq 1$ (and *any* of the two curves $\omega = \omega_{1,2}$ is considered).

The *"pathological"* case (i), which should in principle deserve more tedious analysis, nevertheless only refers to the electrostatic thermal mode in an equal-temperature pair plasma, which – as mentioned above – is known to be an evanescent mode and hardly propagates, in practice, since it is subject to a very strong Landau damping [20]. In other words, the fluid model employed here, which (as long discussed [18-19]) fails to predict Landau damping effects in general, is simply invalidated in Case (i). Therefore, examining this case would be meaningless and is therefore abandoned. Concluding, we shall assume in the following that $\omega^2 \neq \gamma k^2$ *and* $\omega^2 \neq \gamma\sigma k^2$ [i.e. peeking into Cases (i) and (ii) above].

According to the above, either for the upper dispersion branch ω_2, or for the lower one ω_1 for $\sigma \neq 1$ (i.e. $T_- \neq T_+$), the 1st order 1st harmonic amplitudes are determined as

$$n_{-,1}^{(1)} = \frac{k^2}{-\omega^2 + \gamma k^2}\phi_1^{(1)}, \qquad n_{+,1}^{(1)} = \frac{k^2}{\omega^2 - \gamma\sigma k^2}\phi_1^{(1)}, \qquad k\,u_{+,1}^{(1)} = \omega n_{+,1}^{(1)},$$

$$k\,u_{-,1}^{(1)} = \omega n_{-,1}^{(1)}, \qquad u_{-,l}^{(1)} = \frac{k\omega}{-\omega^2 + \gamma k^2}\phi_1^{(1)}, \qquad u_{+,1}^{(1)} = \frac{k\omega}{\omega^2 - \gamma\sigma k^2}\phi_1^{(1)}. \qquad (14)$$

Advancing the analysis to the second-order (n =2) equations, for the 1st harmonics (l=1), the following compatibility condition is obtained

$$\lambda = \frac{\omega}{k} - \frac{1}{k\omega\left[\frac{1}{(\omega^2 - \gamma k^2)^2} + \frac{1}{(\omega^2 - \gamma\sigma k^2)^2}\right]} \quad . \tag{15}$$

It is straightforward to show that $\lambda = v_g(k) = d\omega/dk$, which determines the group velocity.

In the particular case $\sigma = 1$, the latter expression reduces to $v_{g,1} = \sqrt{\gamma}$ and $v_{g,2} = \gamma k/(\gamma k^2 + 2)^{1/2}$. Solving the resulting equations for n=2 and l=0 and 2 we obtain the second harmonic correction amplitudes of the state variables, in addition to a zeroth harmonic (direct current) terms; an arbitrary correction to the first harmonic (for n=2) is set to zero, for simplicity. The corresponding expressions, which have been derived in order to be introduced in subsequent orders in n, are omitted here, for brevity.

Proceeding to n=3, l=1 in Eqs. (8), we obtain a compatibility condition in the form of a nonlinear Schrödinger equation [33]

$$i\,\frac{\partial\psi}{\partial\tau} + P\frac{\partial^2\psi}{\partial\xi^2} + Q|\psi|^2\psi = 0 \quad , \tag{16}$$

which describes the slow evolution of the first-order amplitude of the plasma electric potential perturbation $\psi \equiv \phi_1^{(1)}$. The dispersion coefficient P is related to the dispersion curve as $P = \frac{1}{2}\frac{\partial^2\omega}{\partial k^2}$. Its exact form reads

$$
\begin{aligned}
P = & \frac{(\omega^2 - k\lambda\omega)^2(\omega - k\lambda)}{2\omega^2 k^2}\left[\frac{\omega^2 + \gamma k^2}{(\omega^2 - \gamma k^2)^3} + \frac{\beta(\omega^2 + \gamma\sigma k^2)}{(\omega^2 - \gamma\sigma k^2)^3}\right] \\
& + \frac{\gamma(\omega^2 - k\lambda\omega)^2}{\omega}\left[\frac{1}{(\omega^2 - \gamma k^2)^3} + \frac{\sigma}{(\omega^2 - \gamma\sigma k^2)^3}\right] \\
& - \frac{(\omega^2 - k\lambda\omega)}{2\omega k^2} - \frac{(\omega^2 - k\lambda\omega)^2\lambda}{k}\left[\frac{1}{(\omega^2 - \gamma k^2)^3} + \frac{1}{(\omega^2 - \gamma\sigma k^2)^3}\right] \quad .
\end{aligned} \tag{17}
$$

For $\sigma = 1$ and $\omega = \omega_2$, this expression reduces to $P_2 = \gamma^{1/2} / \left[2k^{1/2}\ (\gamma k^2 + 2)^{5/4}\right] \ > \ 0$. On the other hand, for $\sigma = 1$ and $\omega = \omega_1$, one gets $P_1 = 0$; the fluid model, which is then not valid, as said above, even fails to provide the 2nd order dispersion needed to balance nonlinearity in the NLS equation.

The nonlinearity coefficient Q, which is due to the carrier wave self-interaction, is given by

$$
\begin{aligned}
Q = & -\frac{k^3(2\omega + k\lambda)(\omega^2 - k\lambda\omega)}{2\lambda\omega}\left[\frac{(\omega^2 + 3k^2)}{(\omega^2 - 3k^2)^4} + \frac{(\omega^2 + 3\sigma k^2)}{(\omega^2 - 3\sigma k^2)^4}\right] \\
& - \frac{3k^4(\omega^2 - k\lambda\omega)}{4\omega}\left[\frac{(\omega^2 + 3k^2)(\omega^2 + k^2)}{(\omega^2 - 3k^2)^5} + \frac{(\omega^2 + 3\sigma k^2)(\omega^2 + \sigma k^2)}{(\omega^2 - 3\sigma k^2)^5}\right] \\
& - \frac{3k^4(\omega^2 - k\lambda\omega)}{4\omega}\left[\frac{(\omega^2 + k^2)[\omega^2 + k^2 + 6k^2(\omega^2 - 3k^2)]}{(\omega^2 - 3k^2)^6} + \right. \\
& \left. \frac{(\omega^2 + \sigma k^2)[\omega^2 + \sigma k^2 + 6\sigma k^2(\omega^2 - 3\sigma k^2)]}{(\omega^2 - 3\sigma k^2)^6}\right] + \\
& \frac{3k^4(\omega^2 + k^2)(\omega^2 + \sigma k^2)(\omega^2 - k\lambda\omega)}{2\omega(\omega^2 - 3k^2)^3(\omega^2 - 3\sigma k^2)^3} + \frac{(2k\lambda\omega + \omega^2 + 3k^2)(\omega^2 - k\lambda\omega)}{2\omega[\lambda^2 - 3\sigma + (\lambda^2 - 3)]}\{ \\
& \frac{2\omega k^3(\lambda^2 - 3\sigma - 3) - k^2\lambda(\omega^2 + 3k^2)}{\lambda(\omega^2 - 3k^2)^4} - \frac{4\omega k^3\lambda}{(\omega^2 - 3k^2)^2(\omega^2 - 3\sigma k^2)^2} \\
& - \frac{k^2(2\omega^2 + 3k^2 + 3\sigma k^2)}{(\omega^2 - 3k^2)^2(\omega^2 - 3\sigma k^2)^2} + \frac{2\omega k^3(\lambda^2 - 3\sigma - 3) - k^2\lambda(\omega^2 + 3\sigma k^2)}{\lambda(\omega^2 - 3\sigma k^2)^4}\}
\end{aligned} \tag{18}
$$

where we have set $\gamma = 3$, for simplicity.

For $\sigma = 1$ (equal temperature pair plasma) and $\omega = \omega_2$ (upper dispersive mode), expression (18) simplifies significantly as

$$Q_2\big|_{\sigma=1} = +\frac{k^2\ \left[4+9k^2(7+18k^2+12k^4)\right]}{24\sqrt{2+3k^2}} \quad > \quad 0\,.$$

The numerical value of the coefficients P_2 and Q_2, say, i.e. *P* and *Q* as they result from Eqs. (17) and (18) for $\omega=\omega_2$ and $\sigma=1$, are represented in Figures 2a, b. We note that both coefficients are strictly monotonic positive functions of *k*: in fact, *P > 0* (*Q > 0)* decreases (increases) with *k*, while their (positive) product *PQ* increases with *k* (see. 2c). The ratio *P/Q < 0* decreases, on the contrary, as *k* increases (see Fig. 2d). A similar qualitative picture is obtained for $\sigma<1$; the figures are omitted. It may be interesting to trace the asymptotic behavior of these coefficients for small *k*, i.e. for a large wavelength compared to the Debye radius. In fact, P_2 behaves as $P_2 \approx \frac{\gamma(1+\sigma)}{4\sqrt{2}} - \frac{3\gamma^2(3-\sigma)(3\sigma-1)}{32\sqrt{2}}\ k^2$ for small *k*, while Q_2 goes to zero as $Q_2 \sim \frac{k^2}{3\sqrt{2}\ (1+\sigma)}$ (for $\gamma=3$). The product *PQ* therefore behaves as $\sim k^2$ (prescribing modulational instability, as we shall see), for small *k*, while $P/Q \sim k^{-2}$ in the same limit.

Relying on expressions (17) and (18), one may also compute the coefficients in the NLS equation (16) for the lower (thermal) mode, for $\sigma \neq 1$. Adopting, for instance, as a working hypothesis that positive ions (or positrons) are warmer than negative ions (or electrons), we may set $\sigma=1.5$ (which is physically rather unlikely a situation). The numerical value of the coefficients P_1 and Q_1, i.e. *P* and *Q* as they result from Eqs. (17) and (18) for $\omega=\omega_1$ and $\sigma=1.5$, are represented in Figures 3a, b. The qualitative picture is quite different now: in fact, *P* and *Q* now bear opposite signs for low *k* (in fact, values higher than 1 are strongly damped and need not be considered); see Fig. 3c. The ratio *P/Q* is negative (positive) for low (high) *k*, while its positive value increases for *k* up to 0.8 approximately, and then decreases again (see Fig. 3d). The asymptotic behavior of these coefficients for small *k* is now qualitatively different. In fact, P_1 goes to zero as

$P_1 \sim -\dfrac{3\gamma^{3/2}(1-\sigma)^2}{8\sqrt{2(1+\sigma)}}k \;<\; 0$, while Q_1 diverges as $Q_1 \sim +\dfrac{16\sqrt{2/3}\sqrt{1+\sigma}\,(3+\sigma)}{27(1-\sigma)^4\;k} \;>\; 0$ (for $\gamma = 3$). The product PQ therefore tends to a negative constant, for small k, while $P/Q \sim -k^2 \;<\; 0$ in the same limit. A similar qualitative picture is obtained for $\sigma < 1$ (the corresponding figures are omitted).

IV. Modulational stability analysis

The stability analysis of the NLS equation (16) consists in linearizing around the monochromatic wave solution $\psi = \hat{\psi}\, e^{iQ|\hat{\psi}|^2\tau}$, by setting $\hat{\psi} = \hat{\psi}_0 + \varepsilon\hat{\psi}_1$, and then taking the perturbation $\hat{\psi}_1$ to be of the form $\hat{\psi}_1 = \hat{\psi}_{1,0}e^{i(\hat{k}\xi - \hat{\omega}\tau)}$ (the perturbation wavenumber $\hat{k}$ and frequency $\hat{\omega}$ should be distinguished from the carrier wave quantities k and ω). One thus obtains the dispersion relation $\hat{\omega}^2 = P\,\hat{k}^2\,(P\hat{k}^2 - 2Q|\hat{\psi}_0|^2)$. In order for the wave to be stable, the product PQ *must be negative*. Otherwise, for positive PQ, instability sets in for perturbation wavenumber values below a critical value $\hat{k}_{cr} = \sqrt{2Q/P}\,|\hat{\psi}_0|$, i.e. for wavelength values above the threshold $\lambda_{cr} = 2\pi/\hat{k}_{cr}$. The maximum instability growth rate $\sigma = |\mathrm{Im}\,\hat{\omega}(\hat{k})|$, i.e. $\sigma_{\max} = |\mathrm{Im}\,\hat{\omega}|_{\hat{k}=\frac{\hat{k}_{cr}}{\sqrt{2}}} = |Q||\hat{\psi}_0|^2$, is achieved at $\hat{k} = \hat{k}_{cr}/\sqrt{2}$. We draw the conclusion that the instability condition depends only on the sign of the product PQ, which may now be studied numerically, relying on the exact expressions derived above.

The upper (Langmuir-like dispersive) electrostatic mode $\omega = \omega_2$ defined above is seen to be modulationally *unstable* for a temperature ratio $\sigma = 1$, since the product PQ is positive for this mode, for any value of the wavenumber k, as we have shown above. This qualitative behavior is also valid for σ other than unity, as may be checked either analytically or numerically; nevertheless, the product PQ may change sign for higher k here, stabilizing the upper electrostatic mode; see Fig. 4d.

The lower (thermal) electrostatic mode $\omega = \omega_1$ sign turns out to be modulationally *stable* (*unstable*) for low (high) *k*, since the product *PQ* is negative (positive) in the corresponding wavenumber *k* regions. This qualitative behavior is valid for any value of the temperature ratio $\sigma \neq 1$ (this analysis is not valid for $\sigma = 1$, as explained above). The thermal mode is therefore subject to modulational instability for small wavelengths (in addition to Landau damping, which prevails inevitably).

V. Envelope excitations

The localized solutions of the NLSE (16) describe (arbitrary amplitude) nonlinear excitations, in the form of bright and dark (black/gray) envelope solitons. Exact expressions for these envelope structures can be found by substituting $\phi = \sqrt{\rho}\exp(i\Theta)$ into Eq. (16), and then separating the real and imaginary parts, in order to determine the real functions $\rho = \rho(\xi, \tau)$ and $\Theta = \Theta(\xi, \tau)$. The final formulae are derived in Ref. [34] (also exposed e.g. in [32]), and need therefore only briefly be summarized in the following.

For *PQ*>0 we find the *bright* envelope soliton:

$$\rho = \rho_0 \sec h^2(\frac{\xi - u\tau}{l}) \ , \qquad \theta = \frac{1}{2P}[u\xi - (\Omega + \frac{1}{2}u^2)\tau] \ , \tag{19}$$

which represents a localized pulse traveling at a speed *u* and oscillating at a frequency Ω (at rest). The pulse width l depends on the constant maximum amplitude square ρ_0 as $l = \sqrt{2P/Q\rho_0}$. We note that the maximum amplitude $\sqrt{\rho_0}$ is inversely proportional to the spatial extension l; this is also true in the dark envelope soliton case (see below).

For *PQ*<0 we have the *black* envelope soliton

$$\rho = \rho_1[1 - \sec h^2(\frac{\xi - u\tau}{l'})] = \rho_1 \tanh^2(\frac{\xi - u\tau}{l'}) \ , \qquad \theta = \frac{1}{2P}[u\xi - (\frac{1}{2}u^2 - 2PQ\rho_1)\tau] \ , \tag{20}$$

which represents a localized region of negative wave density perturbation travelling at a speed u. The pulse width depends on the maximum amplitude square ρ_1 via $l' = \sqrt{|2P/Q\rho_1|}$.

Finally, for PQ<0, one also obtains the *gray envelope soliton* excitation, with

$$\rho = \rho_2[1 - a^2 \sec h^2(\frac{\xi - u\tau}{l''})] \ ,$$

and

$$\theta = \frac{1}{2P}[u\xi - (\frac{u^2}{2} - 2PQ\rho_2)\tau + \theta_{10}] - s\sin^{-1}\frac{a\tanh(\frac{\xi - u\tau}{l''})}{[1 - a^2\sec h^2(\frac{\xi - u\tau}{l''})]^{\frac{1}{2}}} \ , \qquad (21)$$

which also represents a localized region of negative wave density, though with a finite (i.e. non-zero, contrary to the black envelope soliton above) amplitude at the origin. Here, θ_{10} is a constant phase, s denotes the product $s = signP \times sign(u - V_0)$. In comparison to the *black* soliton above, note that apart from the maximum amplitude $\sqrt{\rho_2}$, which is now finite everywhere, the pulse width of this gray-type excitation: $l'' = (1/a)\sqrt{2|P/Q\rho_2|}$, now also depends on the dimensionless parameter a, which is given by $a^2 = 1 + (u - V_0)^2/(2PQ\rho_2) \le 1$ (for PQ<0), an independent parameter representing the modulation depth $(0 < a \le 1)$. V_0 is an independent real constant which satisfies the condition $V_0 - \sqrt{2|PQ|\rho_2} \le u \le V_0 + \sqrt{2|PQ|\rho_2}$; for $V_0 = u$, we have a=1 and thus recover the *black* soliton presented in the previous paragraph.

Focusing on our electrostatic pair-plasma mode problem, we notice that the dark (black or grey) type excitations presented above may be relevant to the propagation of waves obeying the lower (ion thermal-like) dispersion mode, since these possess a negative PQ value; cf. Fig. 3c. In this case, the width of the excitations (which, for a given maximum amplitude, is given by the ratio P/Q) will be higher for higher wavenumbers k, i.e. for short wavelengths λ, as shown in Fig. 3d. Of course, the kinetic

Landau damping mechanism here once again overseen somehow invalidates (although does rather not annihilate) these predictions.

On the other hand, the bright type excitations may occur as propagating localized wavepackets obeying the upper (Langmuir-like) dispersion curve, since this one possesses a negative PQ value; cf. Figs. 2c and 4c. In this case, the width of the excitations (which again scales, for a given amplitude, as P/Q) will be narrower for higher wavenumbers k (or lower wavelengths), up to a values of, say, $k \approx 1.5\,\lambda_D^{-1}$), where the product PQ changes sign; cf. Fig. 4d.

VI. Conclusions

In this paper, we have investigated the nonlinear propagation of electrostatic wave packets in pair plasmas, by employing a two-fluid plasma model. Electrostatic mode propagation parallel to the external magnetic field was considered. The temperature ratio among the two species has been left arbitrary in the analysis, although the natural choice of unity was focused upon and discussed extensively. Two distinct electrostatic modes were obtained, namely a quasi-ion-thermal lower mode and a Langmuir-like optic-type upper one, in agreement with previous experimental observations confirmed by theoretical studies of equal-temperature pair plasmas. Considering small yet weakly nonlinear deviations from equilibrium, and adopting a multiple scale technique, the basic set of model equations was reduced to a nonlinear Schrödinger equation for the slowly varying electric field perturbation amplitude.

The analysis revealed that the lower (ion-thermal) mode is stable and may propagate in the form of a dark-type envelope soliton (i.e. a potential dip, or a density void) modulating a carrier wavepacket. On the other hand, the upper mode is modulationally unstable, and may yet favor the formation of bright-type envelope soliton (pulse) modulated wavepackets. Admittedly, Landau damping (inevitably overseen in a fluid model) should also be taken into consideration, with respect to the lower (ion-thermal) mode. As expected, these results depend on the temperature ratio, as one may

see in Fig. 5. In specific, going beyond current experimental considerations, one may anticipate that a local coexistence of positive ions (or positrons) with a colder, say, population of negative ions (or electrons), viz. $\sigma < 1$, may critically affect the stability profile of electrostatic modes, for instance by stabilizing the upper mode (which is unstable near $\sigma = 1$, see Fig. 5c), or by destabilizing the lower mode (which is stable near $\sigma = 1$, see Figs. 5a, b).

These results are relevant to recent observations of electrostatic waves in pair-ion (fullerene) plasmas. Furthermore, this analysis may also be relevant to modulated electron-positron plasma radio emission in pulsar magnetospheres. Our predictions may be investigated, and will hopefully be confirmed, by appropriately designed experiments.

Acknowledgements

I.K. greatfully acknowledges support by the *Deutsche Forschungsgemeinschaft* (Bonn, Germany) through the Programme *Sonderforschungsbereich (SFB) 591 - Universelles Verhalten Gleichgewichtsferner Plasmen: Heizung, Transport und Strukturbildung*.

References

[1] V. L. Ginzburg, Sov. Phys. Usp. **14**, 83 (1971);
P. A. Sturrock, Astrophys. J. 164, 529 (1971).

[2] M. A. Ruderman and P. G. Sutherland, Astrophys. J. **196**, 51 (1975).

[3] R. N. Manchester and J. H. Taylor, Pulsars (Freeman, San Francisco, 1977).

[4] F. C. Michel, Rev. Mod. Phys. **54**, 1 (1982).

[5] F. C. Michel, Theory of neutron Star Magnetospheres (University of Chicago Press, Chicago, 1991); see also in:
S. Johnston, M. A. Walker and M. Bailes (Eds.), Pulsars: Problems and Progress, Astrophysical Society (ASP) of the Pacific Conference Series **105** (ASP, San Francisco, 1996).

[6] H. R. Miller and P. J. Witta, Active Galactic Nuclei (Springer-Verlag, Berlin, 1987), p. 202;
M. C. Begelman, R. D. Blandford and M. D. Rees, Rev. Mod. Phys. **56**, 255 (1984).

[7] M. L. Burns, in Positron-Electron Pairs in Astrophysics (M. L. Burns, A. K. Harding and R. Ramaty, Eds.), (American Institute of Physics, New York, 1983).

[8] G. W. Gibbons, S. W. Hawking and S. Siklos, The Very Early Universe (Cambridge University Press, Cambridge, 1983).

[9] E. P. Liang, S. C. Wilks and M. Tabak, Phys. Rev. Lett. **81**, 4887 (1998);
C. Gahn, G. D. Tsakiris G. Pretzler *et al.*, Appl. Phys. Lett. **77**, 2662 (2000).

[10] P. Helander and D. J.Ward, Phys. Rev. Lett. **90**, 135004 (2003).

[11] C.M. Surko, M. Leventhal and A. Passner, Phys. Rev. Lett. **62,** 901 (1989).

[12] C.M. Surko and T.J. Murphy, Phys. Fluids **2,** 1372 (1990).

[13] R.G. Greaves, M.D. Tinkle and C.M. Surko, Phys. Plasmas **1,** 1439 (1994).

[14] J. Zhao, J. I. Sakai and K. Nishikawa, Phys. Plasmas **3**, 844 (1996).

[15] W. Oohara and R. Hatakeyama, Phys. Rev. Lett. **91,** 205005 (2003).

[16] W. Oohara, D. Date and R. Hatakeyama, Phys. Rev. Lett. **95,** 175003 (2005).

[17] R. Hatakeyama and W. Oohara, Phys. Scr. **116,** 101 (2005).

[18] N.A. Krall and A.W. Trivelpiece, Principles of plasma physics (NewYork, McGraw-Hill, 1973).

[19] T. Stix, Waves in plasmas (New York: American Institute of physics, 1992).

[20] V. Tsytovich and C.B. Wharton, Comm. Plasma Phys. Cont. Fusion **4,** 91 (1978).

[21] N. Iwamoto, Phys. Rev. E **47,** 604 (1993).

[22] J. Vranjes and S. Poedts, Plasma Sources Sci. Technology **14,** 485 (2005).

[23] G.A. Stewart and E.W. Laing, J. Plasma Phys. **47,** 295 (1992).

[24] G.P. Zank and R.G. Greaves, Phys. Rev. E **51,** 6079 (1995).

[25] L. Stenflo, P. K. Shukla and M. Y. Yu, Astrophys. Space Sci. **117**, 303 (1985).

[26] P.K. Shukla, N.N. Rao, M. Yu and N. L. Tsintsadze, Phys. Rep. **138**, 1 (1986).

[27] F. Verheest and G. S. Lakhina, New J. Phys. **7**, 94 (2005).

[28] T. Cattaert, I. Kourakis and P. K. Shukla, Phys. Plasmas **12**, 012319 (2005).

[29] S. I. Popel, S. V. Vladimirov and P. K. Shukla, Phys. Plasmas, **2**, 716, (1995).

[30] T. Taniuti and N. Yajima, J. Math. Phys. **10,** 1369 (1969).

[31] N. Asano, T. Taniuti and N. Yajima, J. Math. Phys. **10,** 2020 (1969).

[32] I. Kourakis and P.K. Shukla, Nonlinear Proc. Geophys., **12**, 407 (2005).

[33] P. Sulem and C. Sulem, Nonlinear Schrödinger Equation (Springer, Berlin, 1999).

[34] R. Fedele, Phys. Scr. **65**, 502 (2002);
R. Fedele, H. Schamel, Eur. Phys. J. B **27,** 313 (2002).

Figure captions

Figure 1.

The two dispersion curves defined by Eq. (13) (for $\sigma = 1$ and $\gamma = 3$) are depicted, as a frequency ω / ω_p variation vs. the reduced wavenumber $k\lambda_D$.

Figure 2.

The (dimensionless) coefficients in the NLS equation, as derived from the upper dispersion branch ω_2, are depicted (for $\sigma = 1$ and $\gamma = 3$) against the reduced wavenumber $k\lambda_D$ (in abscissa everywhere): (a) the dispersion coefficient *P*; (b) the nonlinearity coefficient *Q*; (c) the product *PQ* (whose sign determines the stability profile); (d) the ratio *P/Q* (whose numerical value determines the characteristics of envelope excitations).

Figure 3.

The (dimensionless) coefficients in the NLS equation, as derived from the lower dispersion branch ω_1, are depicted (for $\sigma = 1.5$ and $\gamma = 3$) against the reduced wavenumber $k\lambda_D$ (in abscissa everywhere): (a) the dispersion coefficient *P*; (b) the nonlinearity coefficient *Q*; (c) the product *PQ* (whose sign determines the stability profile); (d) the ratio *P/Q* (whose numerical value determines the characteristics of envelope excitations).

Figure 4.

The (dimensionless) coefficients in the NLS equation, as derived from the higher dispersion branch ω_2, are depicted (for $\sigma = 1.5$ and $\gamma = 3$) against the reduced wavenumber $k\lambda_D$ (in abscissa everywhere): (a) the dispersion coefficient *P*; (b) the nonlinearity coefficient *Q*; (c) the product *PQ* (whose sign determines the stability profile); (d) the ratio *P/Q* (whose numerical value determines the characteristics of envelope excitations).

Figure 5.

The *PQ* =0 contour is depicted against normalized wavenumber k/k_D (in abscissa) and $\sigma = T_-/T_+$. Black/white represents the region where the product *PQ* is negative / positive i.e. the region of modulational stability/instability, which may support dark/bright type solitary excitations: a) the lower dispersion branch ω_1 for $0 \le \sigma \le 0.999$; b) the lower dispersion branch ω_1 for $1.001 \le \sigma \le 2$; c) the higher dispersion branch ω_2 for $0 \le \sigma \le 2$.

Figure 1

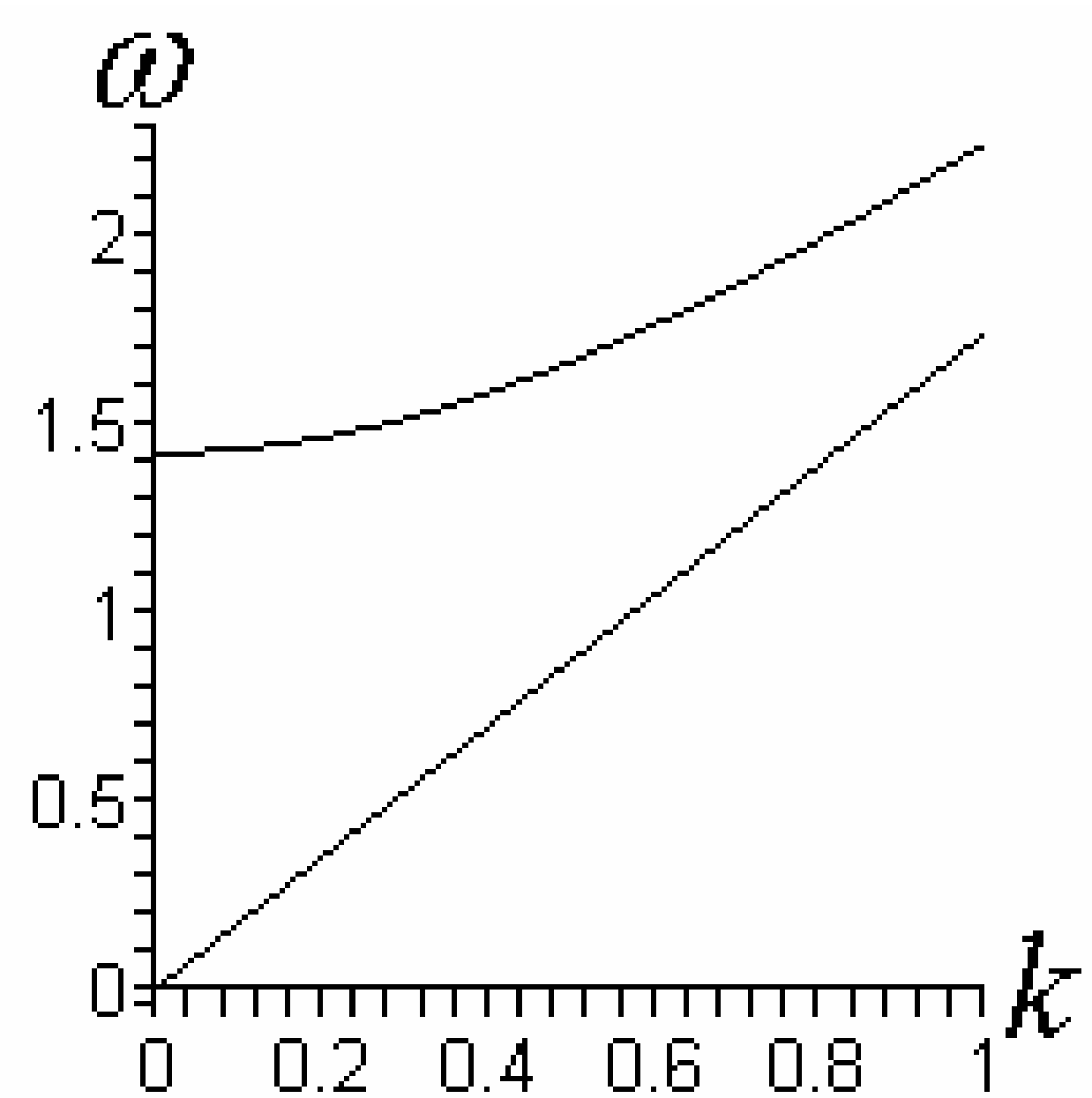

Figure 2

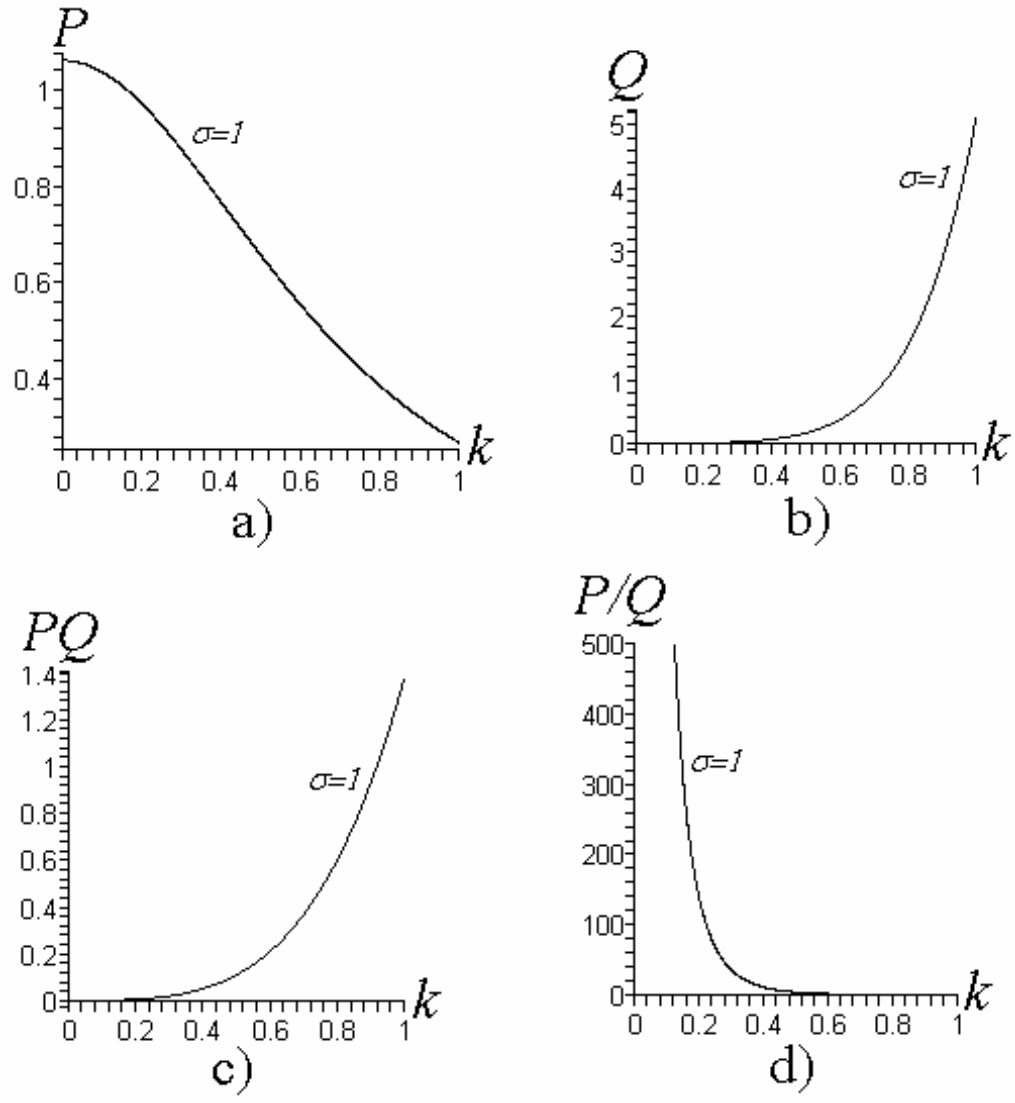
P
1
0.8
0.6
0.4
σ=1
k
0
0.2
0.4
0.6
0.8
1
a)
Q
5
4
3
2
1
0
σ=1
k
0
0.2
0.4
0.6
0.8
1
b)
PQ
1.4
1.2
1
0.8
0.6
0.4
0.2
0
σ=1
k
0
0.2
0.4
0.6
0.8
1
c)
P/Q
500
400
300
200
100
0
σ=1
k
0
0.2
0.4
0.6
0.8
1
d)

Figure 3

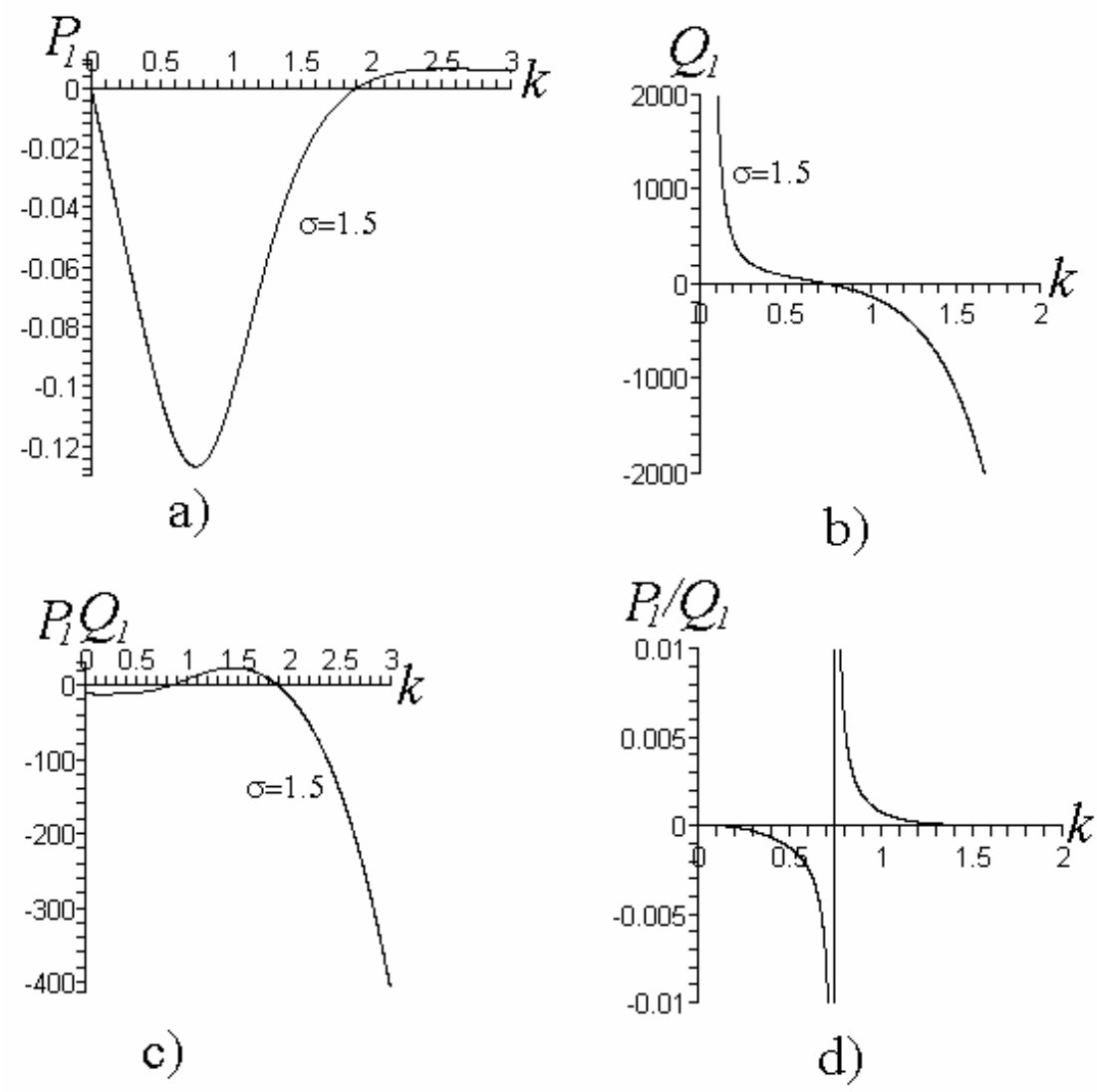

Figure 4

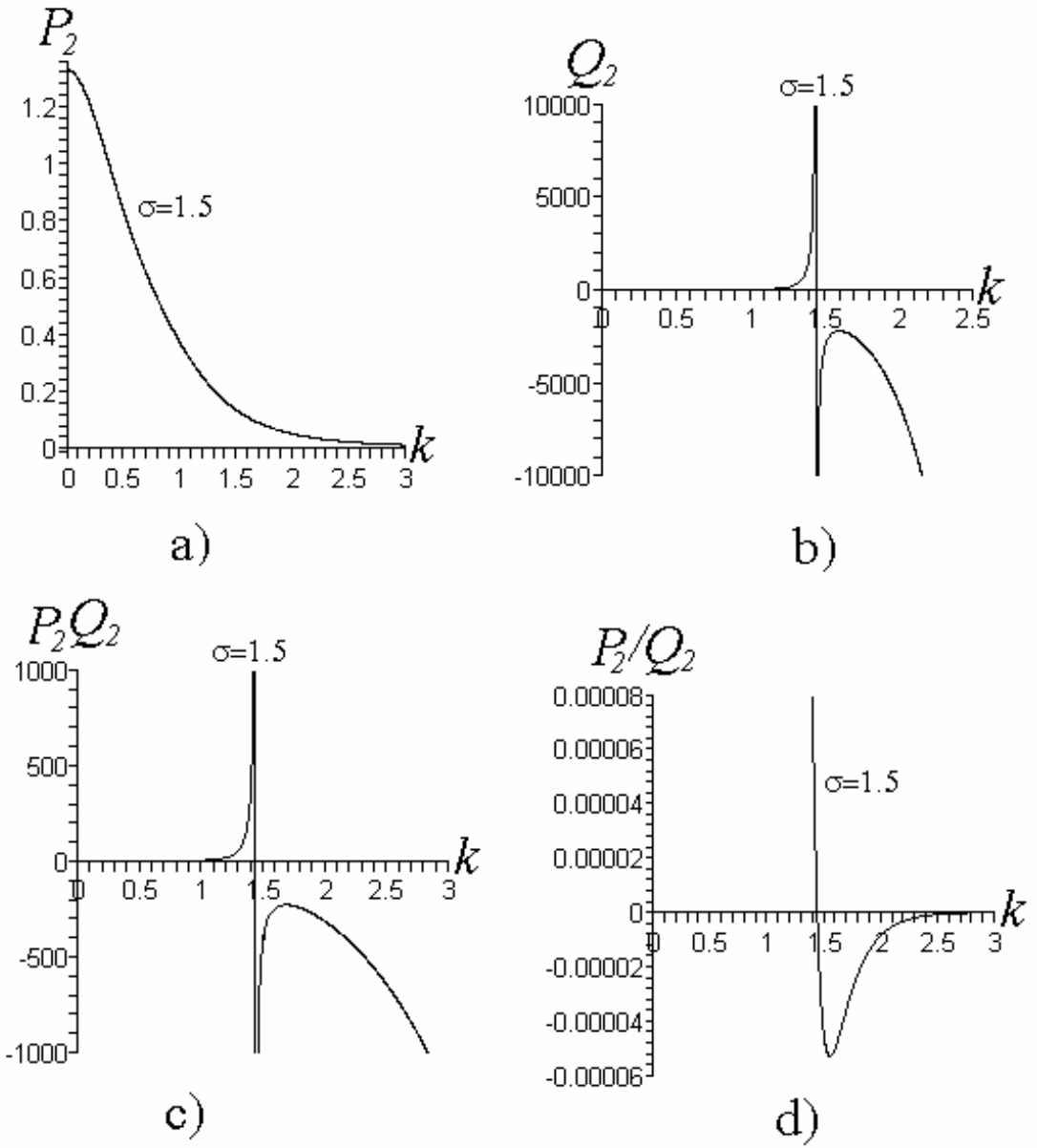

Figure 5

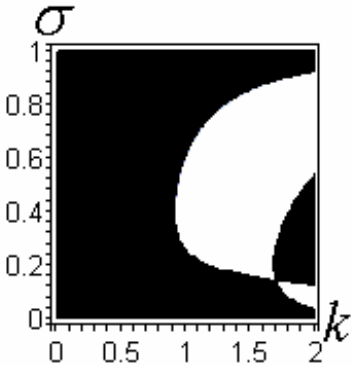
σ
1
0.8
0.6
0.4
0.2
0
k
0
0.5
1
1.5
2

a)

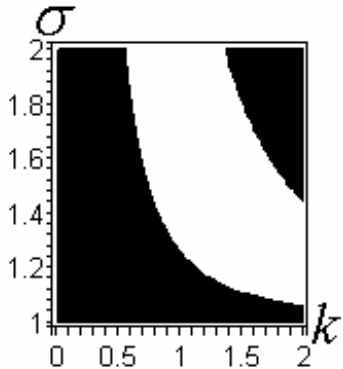
σ
2
1.8
1.6
1.4
1.2
1
k
0
0.5
1
1.5
2

b)

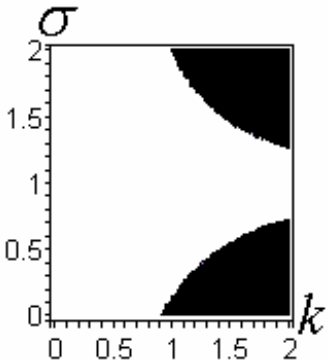
σ
2
1.5
1
0.5
0
k
0
0.5
1
1.5
2

c)